

NOVEL SINGLE-AXIS FLEXURE MECHANISM DESIGNS WITH IMPROVED BEARING STIFFNESS

Shorya Awtar (awtar@umich.edu)

Precision Systems Design Laboratory, Mechanical Engineering
University of Michigan, Ann Arbor, MI 48109

INTRODUCTION AND BACKGROUND

In this paper, we present two new single-axis flexure mechanism designs that overcome the limitations associated with bearing direction error motion and bearing direction stiffness in the traditional parallelogram and double parallelogram flexure designs, respectively [1, 2].

The parallelogram (P) flexure shown in Fig. 1 provides low motion direction stiffness (K_y), relatively high bearing direction stiffness (K_x), but also exhibits considerable bearing direction error motion (E_x). Assuming the Motion Stage and Ground to be perfectly rigid:

$$K_y = \frac{2EI_1}{L_1^3} k_{11}^{(0)} \quad \text{Eq. (1)}$$

$$K_x = \frac{2EI_1}{L_1^3} \frac{k_{33}}{\left(1 + k_{33} g_{11}^{(1)} \left(\frac{Y}{L_1}\right)^2\right)} \quad \text{Eq. (2)}$$

$$E_x = -\frac{k_{11}^{(1)} Y^2}{2 L_1} \quad \text{Eq. (3)}$$

Here, L_1 is beam length, E is the Young's Modulus, I_1 is the second moment of area in bending, and Y is the motion direction displacement. The non-dimensional coefficients $k_{11}^{(0)}$, $k_{11}^{(1)}$, $g_{11}^{(1)}$, and k_{33} are all functions of the beam shape a_o shown in Fig. 1 and the in-plane beam thickness T_1 , as shown in [2]:

$$k_{11}^{(0)} = \frac{6}{(3 - 6a_o + 4a_o^2)a_o}$$

$$k_{11}^{(1)} = \frac{3(15 - 50a_o + 60a_o^2 - 24a_o^3)}{5(3 - 6a_o + 4a_o^2)^2}$$

$$g_{11}^{(1)} = \frac{2a_o^3(105 - 630a_o + 1440a_o^2 - 1480a_o^3 + 576a_o^4)}{175(3 - 6a_o + 4a_o^2)^3}$$

$$k_{33} = \frac{6}{a_o(T_1/L_1)^2}$$

When $a_o = 0.5$, which corresponds to uniform thickness beams, these coefficients assume the values of 12, 1.2, 1/700, and $12(L_1/T_1)^2$, respectively. As seen in Eqs. (1) and (2), while K_y remains constant with increasing Y displacement,

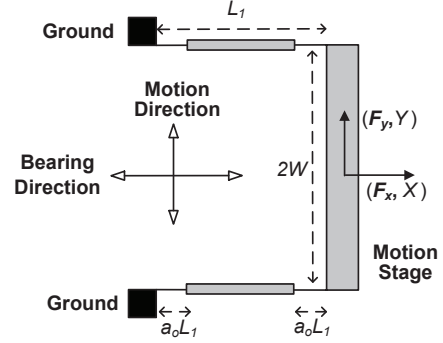


Figure 1. Parallelogram (P) Flexure

K_x gradually drops. This drop is dictated by the elastokinematic effect, which is quantitatively captured by the coefficient $g_{11}^{(1)}$ [1, 2]. This coefficient and therefore the K_x drop can be reduced by optimizing the beam shape via parameter a_o . In general, it is desirable to maximize the bearing direction stiffness (K_x) and minimize the motion direction stiffness (K_y); therefore, the ratio K_x/K_y is plotted in Fig. 2 for $a_o = 0.5$ and 0.2 , with $L_1 = 1000 \mu\text{m}$, $T_1 = 3 \mu\text{m}$, out-of-plane thickness $H_1 = 50 \mu\text{m}$, $W = 400 \mu\text{m}$, and $E = 169\text{GPa}$.

The error motion given in Eq. (3) is fundamental to the kinematics of the P flexure design, causing the Motion Stage to trace a roughly parabolic trajectory instead of a straight line. It arises from beam arc length conservation, which is quantitatively captured by the coefficient $k_{11}^{(1)}$ and cannot be eliminated by beam shape optimization [1, 2]. This

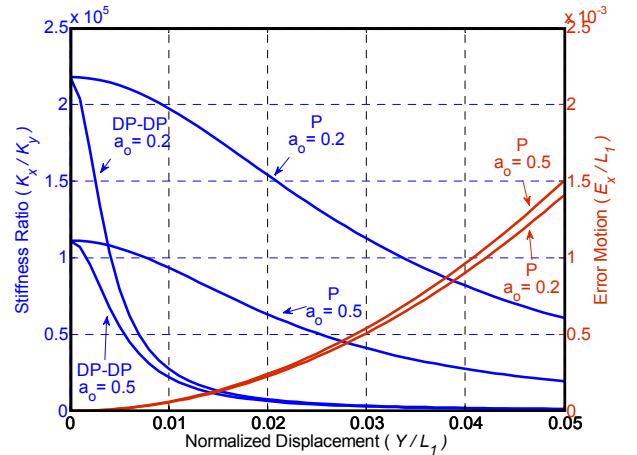


Figure 2. P and DP-DP Flexure Performance

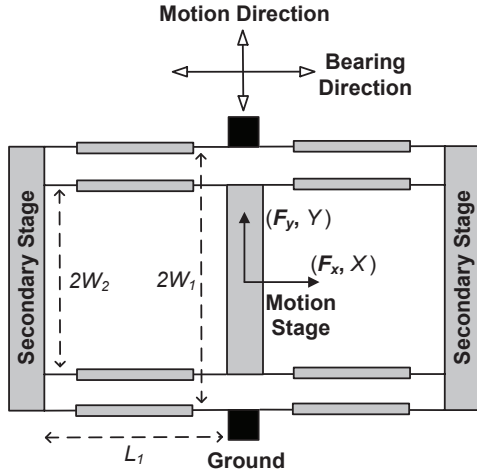


Figure 3. Paired Double Parallelogram (DP-DP) Flexure

error motion is shown in Fig. 2, and proves to be undesirable in certain applications [3].

This error motion is entirely canceled out, in theory, by geometric reversal in the double parallelogram (DP) flexure as well as its paired version (DP-DP) shown in Fig. 3. However, both the DP and DP-DP designs suffer from a precipitous drop in the bearing direction stiffness with motion direction displacement (Y). For the DP-DP flexure design, the bearing direction stiffness is given by:

$$K_x = \frac{2EI_1}{L_1^3} \frac{k_{33}}{\left(1 + \frac{k_{33} (k_{11}^{(1)})^2}{k_{11}^{(0)}} \left(\frac{Y}{2L_1}\right)^2\right)} \quad \text{Eq. (4)}$$

Unlike the P flexure, here the drop in K_x is dictated by the relatively large kinematic coefficient $k_{11}^{(1)}$, which is fundamental to the beam and cannot be reduced much via beam shape optimization. However, the motion direction stiffness (K_y) of the DP-DP flexure remains the same as that of the P flexure, and fairly constant with Y displacement. With the previous dimensions and $W_1 = 500 \mu\text{m}$ and $W_2 = 400 \mu\text{m}$, the resulting K_x/K_y ratio for the DP-DP flexure is also plotted in Fig. 2 for $a_0 = 0.2$ and 0.5 . In the latter case, when going from $Y = 0$ to $Y = 0.01L_1$, the K_x stiffness drops by 80% for the DP-DP flexure, compared to 16% for the P flexure.

The large drop in bearing stiffness is explained by the fact that the DP flexure geometry represents a kinematically under-constrained design [1, 2, 4-6]. When its Motion Stage is held fixed at a non-zero Y displacement, its Secondary Stage moves by $Y/2$ but remains kinematically free in the motion direction. Therefore, when a bearing direction force F_x is applied on the Motion Stage, the load-stiffening and load-softening effects in the flexure's constituent beams causes the Secondary Stage to

move additionally from its nominal $Y/2$ displacement. This additional displacement of the Secondary Stage leads to a disparity between the geometric contraction of the constituent beams along their length, thus producing an additional displacement at the Motion Stage and therefore an additional compliance in the bearing direction. In the DP-DP flexure, both the Secondary Stages are under-constrained. Upon the application of a bearing force F_x , when Motion Stage is displaced by Y , both Secondary Stages move from their nominal $Y/2$ displacement by equal and opposite amounts. An analytical derivation of how this under-constrained behavior affects the bearing direction stiffness is presented in [1, 2].

In this paper, we present two new flexure designs, both based on the DP-DP layout that appropriately constrain the redundant motion of the Secondary Stage, thereby improving the bearing stiffness significantly while maintaining E_x close to zero.

PRIOR ART

The problem of under-constraint in the DP flexure geometry was originally reported by Plainvaux [4] and Jones [5], and subsequently by Awtar [1, 2] and Brouwer [6] among others. While Plainvaux [4] recommended the use of gearing to enforce a 1:2 displacement ratio between the Secondary Stage and Motion Stage of the DP flexure, Jones [6] accomplished this "slaving" of the Secondary Stage via a lever mechanism. A monolithic, flexure-based implementation of this lever solution has been implemented by German [7] and Brouwer [8]. These designs indeed produce the desired improvement in the bearing stiffness of the DP.

A separate approach of pre-tilting or pre-bending the beams of a DP or DP-DP flexure mechanism has been common in the design of MEMS electrostatic actuators [3]. This design variation does not mitigate the drop in K_x stiffness with increasing Y displacement; instead, it shifts the location of the K_x stiffness peak in Fig. 2.

CLAMPED DP-DP FLEXURE DESIGN

In the proposed Clamped Paired Double Parallelogram (C-DP-DP) flexure mechanism, shown in Fig.4, the two Secondary Stages are connected to an external clamp via secondary parallelogram (P) flexures. The high rotational stiffness of these P flexures (provided by an appropriate choice of beam separation W_3) suppresses any relative motion direction displacement between the two Secondary Stages, forcing them to maintain $Y/2$ displacement at all times. This constrains these stages from responding to an F_x force on the Motion Stage. Also, the beam length L_3 and in-plane thickness T_3 in the secondary parallelogram

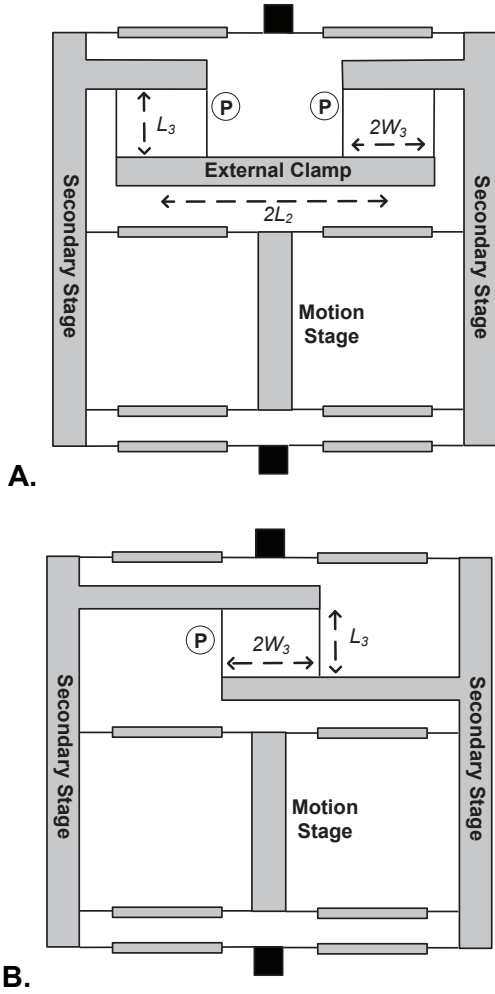


Figure 4. Clamped Paired Double Parallelogram (C-DP-DP) Flexure

flexures are chosen such that they offer minimal resistance to the bearing direction kinematic displacement of the Secondary Stages. This ensures that the motion direction stiffness (K_y) of the C-DP-DP flexure remains the same as that of the DP-DP flexure. However, with the Secondary Stages appropriately constrained, the bearing direction stiffness shows remarkable improvement.

It has been analytically shown that the effectiveness of the clamp is given by the dimensionless parameter η , given by [9]:

$$\eta = \left(\frac{6W_3^2 L_1^3 T_3}{k_{11}^{(0)} L_2^2 L_3 T_1^3} \right)$$

where dimensions are as shown in Figs. 3 and 4. The effect of η on bearing stiffness is shown in Fig. 5 for $a_o = 0.5$ and other dimensions being same as earlier. When L_3 is sufficiently long (typically within $0.5 L_1$) and η is in the range of 100 or greater, the motion and bearing direction stiffness values for the C-DP-DP flexure are given by:

$$K_y = \frac{2EI_1}{L_1^3} k_{11}^{(0)} \quad \text{Eq. (5)}$$

$$K_x = \frac{2EI_1}{L_1^3} \frac{k_{33}}{\left(1 + k_{33} g_{11}^{(1)} \left(\frac{Y}{2L_1} \right)^2 \right)} \quad \text{Eq. (6)}$$

Thus, the bearing stiffness drop is now dictated by the relatively weak elastokinematic coefficient $g_{11}^{(1)}$, which can be reduced via beam shape optimization (a_o). K_x/K_y stiffness ratio for the C-DP-DP flexure, with $\eta = 575$, is plotted in Fig. 5 for $a_o = 0.2$ and 0.5 . In the latter case, from $Y = 0$ to $Y = 0.01L_1$, the K_x stiffness drops by only 4.5%. E_x in this design remains theoretically zero.

As earlier, the above relations assume that all the components of the mechanism other than the beam flexures are perfectly rigid. Another variation of the C-DP-DP design, shown in Fig. 4b, offers similar improvement in bearing stiffness. Obviously, the C-DP-DP design takes up a larger foot-print, which should be optimized for a given application.

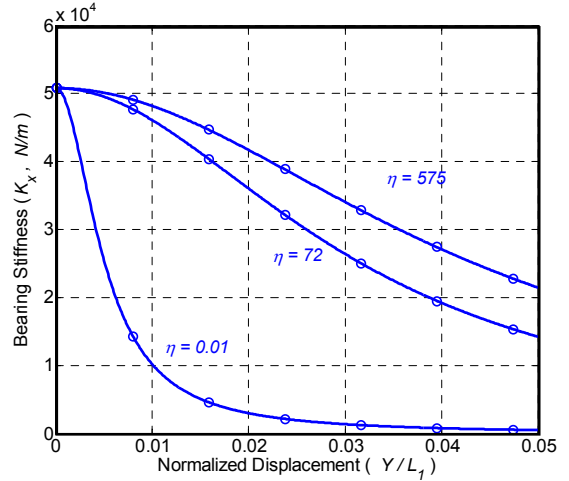


Figure 5 C-DP-DP bearing stiffness: Analytical results (solid lines) and FEA (circles)

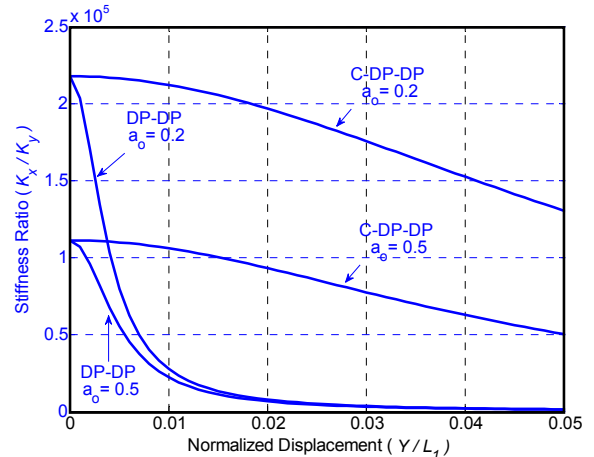


Figure 6 C-DP-DP Flexure Performance

ASYMMETRIC DP-TDP FLEXURE DESIGN

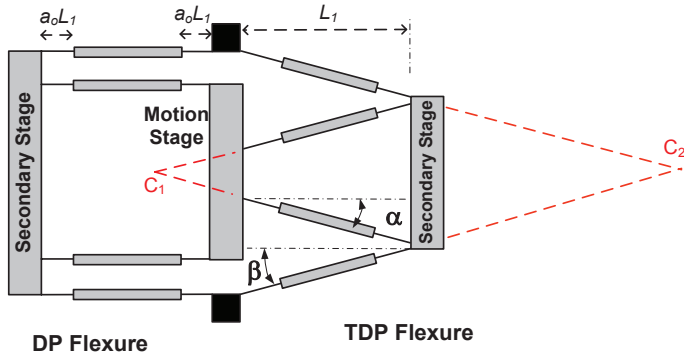


Figure 7. DP-TDP Flexure

The proposed asymmetric Double Parallelogram – Tilted-beam Double Parallelogram (DP-TDP) flexure (Fig. 7) employs a non-intuitive geometric arrangement to kinematically constrain the Secondary Stage of the TDP. The geometry of the TDP module on the right side of Fig. 7 ensures that when the Y and θ displacements of the Motion Stage are specified, there are two conflicting instantaneous centers of rotation (C_1 and C_2) created for its Secondary Stage. However, for this to happen, the θ rotation of the Motion Stage has to be specified, ideally to zero. This is not the case for a TDP by itself, which exhibits finite θ rotation. Therefore, to constrain this θ rotation to approximately zero, a DP flexure is employed on the left side. Thus, the TDP and DP flexures, when coupled together, serve distinct but highly complementary roles. Even though not good with K_x stiffness, the DP flexure provides a high rotational stiffness which constrains the rotation of the combined Motion Stage. This rotational constraint, in turn, ensures that the Secondary Stage of the TDP is kinematically constrained such that its motion direction displacement remains approximately half that of the Motion Stage. This

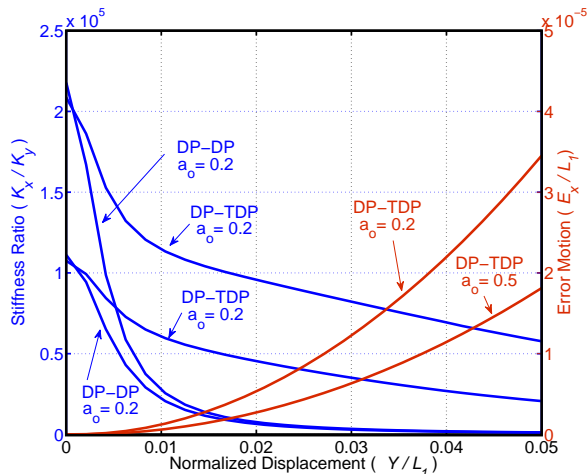


Figure 8 DP-TDP Flexure Performance

provides the desired improvement in the K_x stiffness behavior of the overall DP-TDP flexure. With suitable choice of angles α and β , the overall K_y stiffness can be maintained at the same level as the DP-DP flexure and the error motion E_x can be maintained close to zero [9]. One optimal combination of α and β is 0.11 and 0.14, respectively.

Closed-form analysis of the DP-TDP design is relatively more complicated. Instead, with same dimensions as earlier, FEA prediction of the K_x/K_y ratio are provided in Fig.8 for $a_0 = 0.2$ and 0.5. In the latter case, from $Y = 0$ to $Y = 0.01L_1$, the K_x stiffness drops by 45%. E_x in this design is two orders of magnitude less than the P flexure. The DP-TDP flexure covers approximately the same foot-print as the DP-DP flexure.

RESULTS AND CONCLUSION

All closed-form analytical results presented here have been validated via FEA, which was conducted in ANSYS using BEAM4 elements for the flexures and MPC184 for the rigid stages. Large displacement option (NLGEOM) was turned on. The C-DP-DP and DP-TDP flexures have been separately incorporated within MEMS electrostatic actuators, which experimentally demonstrated large strokes and confirmed the high bearing stiffness. A macro-scale experimental set-up has been assembled to measure the predicted stiffness values, which is work in progress.

REFERENCES

- [1] S. Awtar, "Synthesis and Analysis of Parallel Kinematic XY Flexure Mechanisms", Sc.D. Thesis, Massachusetts Institute of Technology, 2003
- [2] S. Awtar, "Characteristics of Beam-based Flex-ure Modules", *ASME J. Mech. Des.*, vol.129, 2007
- [3] J.D. Grade, et al., "Design of Large Deflection Electrostatic Actuators," *ASME/IEEE J. MEMS*, vol.12, 2003
- [4] J.E. Plainevaux, "Mouvement Parasite Vertical Dune Suspension Elastique Symetrique a Compensation et Asservissement", *Nuovo Cimento*, vol.11, 1954
- [5] R.V. Jones and I.R. Young, "Some Parasitic Deflexions in Parallel Spring Movements," *J. Scientific Instruments*, vol.33, 1956
- [6] D.M. Brouwer, "Design Principles for Six Degrees-of-freedom MEMS-based Precision Manipulators," Ph.D. Thesis, University of Twente, 2007
- [7] J.H. Jerman, et al., "Miniature Device with Translatable Member", US Patent 6664707, 2003
- [8] D.M. Brouwer, et al., "Long-range Elastic Guidance Mechanisms for Electrostatic Comb-drive Actuators," Proc. EUSPEN International Conference, Delft, Netherlands, 2010
- [9] S. Sood, "Analysis of Single Axis Flexure Bearings Approaching Ideal Bearing Characteristics", M.S. Thesis, University of Michigan, Ann Arbor, 2013